EVALUATING PIXEL-BASED AND OBJECT-BASED APPROACHES FOR FOREST ABOVE-GROUND BIOMASS ESTIMATION USING A COMBINATION OF OPTICAL, SAR, AND AN EXTREME GRADIENT BOOSTING MODEL

Haifa Tamiminia [a, *], Bahram Salehi [a], Masoud Mahdianpari [b], Colin M. Beier [c], Lucas Johnson [d]

[a] Department of Environmental Resources Engineering, State University of New York College of Environmental Science and Forestry (SUNY-ESF), NY 13210, USA - (htamimin, bsalehi)@esf.edu

[b] C-CORE and Department of Electrical and Computer Engineering, Memorial University of Newfoundland, St. John's, NL A1B 3X5, Canada - masoud.mahdianpari@c-core.ca

[c] Sustainable Resources Management, State University of New York College of Environmental Science and Forestry (SUNY-ESF), NY 13210, USA - cbeier@esf.edu

[d] Graduate Program in Environmental Science, State University of New York College of Environmental Science and Forestry (SUNY-ESF), NY 13210, USA - ljohns11@esf.edu

Commission III, WG III/10

KEY WORDS: Extreme gradient boosting (Xgboost), forest biomass, Object-based image analysis (OBIA), Synthetic aperture radar (SAR), Machine learning, Airborne light detection and ranging (LiDAR).

ABSTRACT:

The above-ground biomass (AGB) estimation monitoring provides a powerful tool for the assessment of carbon emission and sequestration. Using remote sensing technique is an environmentally friendly way of biomass estimation. Thus, this paper investigated optical (i.e. Landsat 8 OLI and Sentinel-2), synthetic aperture radar (SAR) (global phased array type L-band SAR (PALSAR/PALSAR-2) and Sentinel-1), and their integration for AGB estimation of the Pack demonstration forest in Warrensburg, NY. Importantly, a LiDAR AGB raster of the study area was used as reference data for training/testing purposes. Then, an extreme gradient boosting (Xgboost) machine learning model was used to predict biomass values. The major goal of this study was to compare the performance of pixel-based and object-based image analysis (OBIA) for the AGB estimation. Results indicated that the object-based approach improved the RMSE of AGB prediction about 6.28 Mg/ha for optical + SAR, 6.17 Mg/ha for SAR, and 5.6 Mg/ha for optical data in comparison to the pixel-based approach. Moreover, the combination of optical and SAR data increased the prediction accuracy regardless of feature extraction approach.

1. INTRODUCTION

Sustainable forest management is a critical topic which contributes to ecological, economical, and socio-cultural aspect of the environment (Siry, Cubbage, and Ahmed 2005). Sustainable and effective forest management requires accurate, consistent and timely forest monitoring. Forests play important role in global ecosystems. In recent years, human and natural effects endanger forests across the globe. Forest disturbance contributes to climate change, decrease biological diversity, disturb hydrological cycles, and causes soil erosion and degradation (Watson et al. 1998). In particular, forest above-ground biomass (AGB) is a crucial parameter in carbon sequestration and climate change issues (M. Li, Im, and Beier 2013). Thus, an accurate method for AGB estimation is required to monitor carbon stocks.

Recently, there has been growing interest in determining AGB in a timely manner using less destructive and cost-effective ways. The traditional field measurement techniques calculate the AGB by cutting and weighing the trees (Silveira et al. 2019). Although this method provides accurate AGB estimation, it requires a lot of labor, cost, and time and it cannot be applied over large areas (M. Li, Im, and Beier 2013). On the other hand, remote sensing techniques are a cost-effective way that can provide valuable

information for AGB estimation over large areas and in a timely manner (Y. Li et al. 2019). Previous studies have emphasized on the high correlation of remote sensing data and AGB which can be used for accurate biomass prediction (Deng et al. 2014; Y. Li et al. 2019). Therefore, this study tries to take advantage of different optical and synthetic aperture radar (SAR) imagery for forest AGB estimation.

Airborne light detection and ranging (LiDAR) is an active optical remote sensing source which provides information on vertical structure of forests (Boudreau et al. 2008; Wulder et al. 2013). Nonetheless, collecting airborne LiDAR data is costly and it is not applicable for large regions. Spaceborne optical and SAR data can be considered alternative useful sources for AGB estimation. Optical imagery have a relatively high correlation with vegetation density, biomass, and chlorophyll content (Yue et al. 2019). However, being sensitive to weather condition and saturation issues in forests with high biomass are their limitations (Zhang et al. 2019). To overcome the problem of severe weather condition, SAR sensors which work at longer wavelength are other options. SAR data may also have limitations with saturation depending on the wavelength and biomass density

---

* Corresponding Author

(Urbazaev et al. 2018). Thus, the combination of multiple remote sensing datasets results in reducing limitations exist in each single source. To date, some studies have focused on using different sources of remote sensing data and their combination for AGB estimation (Boudreau et al. 2008; Karlson et al. 2015; Dube et al. 2016; Berninger et al. 2018; Cao et al. 2018; Dang et al. 2019; Duncanson et al. 2020; Issa et al. 2020; Li et al. 2020). Besides having useful dataset, AGB estimation requires an effective regression model to predict biomass accurately. Traditional statistical models such as linear regressions have been widely used for AGB estimation (Næsset 2011; Li et al. 2020; Zhu et al. 2020). The disadvantage of linear regression models is that they are not suitable for non-linear distributed datasets. Machine learning techniques are one the most well-known models that can cope with non-linear characteristics of remote sensing data (Y. Li et al. 2019). Among machine learning models, decision tree-based algorithms presented better performance in AGB estimation (Y. Li et al. 2019). Since random forest (RF) regression model has been widely explored for predicting AGB values, this study investigates the performance of extreme gradient boosting (Xgboost) machine learning algorithm for AGB estimation. In addition, most of the studies have focused on pixel-based feature extraction approach. This paper with the goal of forest AGB estimation in one of temperate forests of New York State, USA, attempts to use Xgboost technique to model the biomass. Optical (i.e. Landsat 8 OLI and Sentinel-2) imagery, SAR (global phased array type L-band SAR (PALSAR/PALSAR-2) and Sentinel-1) datasets, and the combination of optical and SAR data were used to evaluate the efficiency of different remote sensing sources. However, the primary objective of this paper is to compare the results of pixel-based and object-based image analysis (OBIA) approaches for AGB estimation. OBIA technique has not been explored and its capabilities need to be evaluated.

In this study, we wanted to investigate the potential of OBIA and compare its results with the conventional pixel-based approach. It is worth mentioning that object-based method can overcome the mixed pixel problem by categorizing similar pixels into objects. However, the accuracy of the object-based approach is influenced by the results of the segmentation algorithm. Thus, each method has its own pros and cons while the hypothesis is that the OBIA can provide better estimates.

2. STUDY AREA AND DATA

2.1 Study Area

The study area, the Pack demonstration forest (PDF), covers an area of approximately 2,500 ha which is located in the southern Adirondacks outside the town of Warrensburg, NY (Figure 1). It includes several wetland areas, coniferous forests, deciduous forests and unique ice meadows that make PDF a testament to the area's diversity. PDF elevation ranges from 204 m to 377 m above mean sea level with a mean annual temperature of 5.07°C, and mean annual precipitation of 1158 mm.
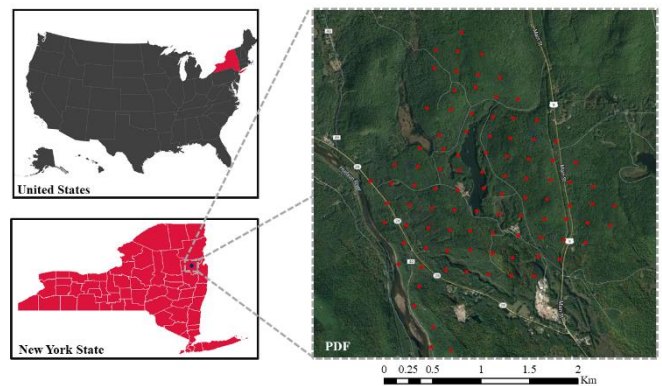

Figure 1. Location of the study area (Warren, NY). Red circles indicate sample plots located in Pack demonstration forest (PDF).

2.2 Field Inventory Data Collection

The State University of New York, College of Environmental Science and Forestry (SUNY-ESF) collected continuous forest inventory (CFI) field measurements. Field data in Pack forest includes 95 sample plots with the radius of 11.33 m (area: 403.33 m^2) were collected in July and August of 2013. The sampling technique was done using a systematic approach as shown in Figure 1. For each sample plot tree species and diameter at breast height (DBH) of 9.14 cm or greater have been recorded. Sample plots consists of northern hardwood species such as acer saccharum (sugar maple), acer rubrum (red maple), betula alleghaniensis (yellow birch), fagus (beech), Fraxinus Americana (white ash), Quercus rubra (red oak), Pinus strobus (white pine), Conium maculatum (hemlock), Picea rubens (red spruce), and Pinus (pine)/softwood plantations of various species (Breitmeyer et al. 2019). The component ratio method (CRM) species-specific allometric equations were used to calculate the AGB for each plot (Woodall et al. 2011; Clough et al. 2018). AGB at PDF ranges from 72.32 to 416.03 Mg/ha with an average of 191.35 Mg/ha with a standard deviation of 66.87 Mg/ha.

2.3 Remote Sensing Data

2.3.1 Airborne LiDAR: Aerial LiDAR data was acquired by New York State GIS program office (NYSGPO) over the study area in 2015. A Leica Airborne Laser Scanner 70 (ALS70) at a maximum flying height of 3500 m above ground level was used to collect discrete returns. First, raw point clouds were converted into height-normalized point clouds. Then, a k-nearest neighbour imputation algorithm ($k = 5$) was used to interpolate a digital elevation model (DEM) which was subtracted from all returns in the point cloud (Hawbaker et al. 2009; Huang et al. 2019). Finally, height (e.g. height, coefficient of variation of height) and intensity (e.g. percentage of ground intensity, percentage of feature intensity) predictors were calculated to generate the AGB raster at 30 m grid cells of the Pack forest. The choice of 30 m grid cells was primarily based on Landsat spatial resolution and to reduce unnecessary computational processing.

2.3.2 Optical Data: The Google Earth Engine (GEE) cloud platform (Gorelick et al. 2017) was used to pre-process and download the imagery. Optical images such as Landsat and Sentinel-2 were used in this research. The datasets were used to extract spectral bands and to calculate 13 vegetation indices. Landsat 8 OLI surface reflectance data of July and August of 2013 were downloaded including Blue, Green, Red, near-infrared (NIR), and two short-wave infrared (SWIR) bands with 30 m resolution (Hemati et al. 2021).

In addition, top of atmosphere reflectance Sentinel-2 multi-spectral instrument (MSI) images of July and August of 2016 were used. Sentinel-2 dataset contains three spectral bands (Red, Green, Blue) (10 m), one NIR (10 m), four red-edge (20 m), and two SWIR bands (20 m) (Earth Resources Observation And Science (EROS) Center 2017). All input layers were resampled using bicubic interpolation and re-projected to NAD83 Conus Albers EPSG: 5070 coordinate system to be aligned with 30 m LiDAR raster.

2.3.3 SAR Data: The global phased array type L-band SAR (PALSAR/PALSAR-2) and Sentinel-1 datasets were acquired from GEE. The dual polarization (horizontal transmit/horizontal receive (HH) and horizontal transmit/vertical receive (HV) polarizations) global PALSAR/PALSAR2 yearly mosaic with 25 m resolution at L-band for 2013 was used. Then, a smoothing speckle filter was applied to the bands to remove the speckle noise (Lee, Grunes, and De Grandi 1999). HH, HV backscatters along with span and ratio were utilized as input predictors for the regression model (Equations 1 and 2).

$$Span = HH^2 + HV^2 \qquad (1)$$

$$Ratio = {HH}/{HV} \qquad (2)$$

where   HH= horizontal transmit/horizontal receive channel
HV = horizontal transmit/vertical receive channel

Sentinel-1 dual polarization C-band data with 10 m resolution was also used. Collection of images in July and August of 2015 in vertical transmit/vertical receive (VV) and vertical transmit/horizontal receive (VH) polarizations was used to estimate AGB. Similar to PALSAR/PALSAR-2 yearly mosaic, a smoothing speckle filter with window size of 3 ×3 was applied and images were resampled into 30 m resolution. In addition to VV and VH bands, span and band ratios were calculated (Lee and Pottier 2009). The images were resampled using bicubic interpolation and reprojected to NAD83 Conus Albers EPSG: 5070 coordinate system to be aligned with 30 m LiDAR raster and optical data.

3. METHODOLOGY

Figure 2 shows an overview of the methods used in this study. First, airborne LiDAR data was used to generate AGB raster of the PDF forest. Second, optical and SAR predictors were extracted from different sensors. Then, Xgboost model was implemented in the R software. For the OBIA, the simple non-iterative clustering (SNIC) algorithm in GEE was used to obtain the objects' boundaries. Objects were exported as shapefiles for the rest of the process in the R software. Finally, the AGB estimates of the PDF forest were compared using the Xgboost model.
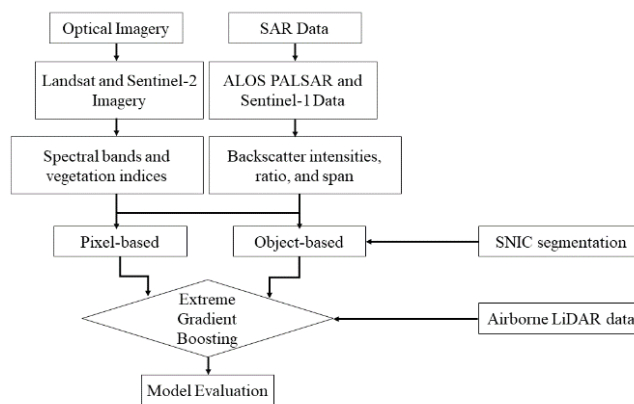

Figure 2. An overview of the methodology used in the study for AGB estimation.

3.1 Extreme Gradient Boosting (Xgboost)

Xgboost is an improved version of gradient boosting machine (GBM) proposed by Chen and Guestrin (2016). It optimizes the objective function by using a second-error Taylor expression while the GBM utilizes the first-order derivatives (Pan 2018; Pesantez-Narvaez, Guillen, and Alcañiz 2019). Regularization, tree pruning, and parallelism are some of the advantages of Xgboost model (Jafarzadeh et al. 2021). Using second derivative enables Xgboost to be faster from a computational speed perspective (Pan 2018). Moreover, regularization can handle both under and over-fitting issues (Li et al. 2020; Pham et al. 2020). These characteristics put Xgboost among the most desirable boosting machine learning algorithms for classification, regression, and ranking tasks (Jafarzadeh et al. 2021).

The "xgboost" package in R software (Chen et al. 2021) was used to implement the Xgboost regression model. Table 1 lists the parameters, their description, and the range of selected values for hyperparameter tuning for Xgboost machine learning model. It should be noted that Xgboost is sensitive to hyperparameter tuning and it might affect its performance (Li et al. 2020). A grid search approach was used for tuning the machine learning parameters.

Parameter	Description	Values
nrounds	the number of rounds for boosting	10, 50, 100, 500, 750, 1000
max_depth	the maximum depth of the tree	from 2 to 10 (with 2 steps)
eta	the step size shrinkage (helps reducing over-fitting)	0 to 1 (with 0.1 step)
gamma	the minimum loss reduction (helps splitting on a leaf node of a tree)	0 to 1 (with 0.1 step)
subsample	the ratio of the subsample for each training cases	0.6 to 1 (with 0.1 step)
min_child_weight	the minimum sum of sample weight required to be in each node	1 to 5 (with 1 step)

Parameter	Description	Values
learning_rate	the weighting of new trees	0.01, 0.05, 0.1, 0.2, and 0.3

Table 1. Parameters for hyperparameter tuning of Xgboost regression model in R software.

3.2 LiDAR AGB raster as reference data

As mentioned earlier, PDF forest includes 95 sample plots. To increase the number of training/testing samples for implementing the machine learning model, LiDAR-derived AGB raster can be used as a reference data. Several studies used this technique for forest AGB estimation using remote sensing datasets (Hirata et al. 2018; Hudak et al. 2020).

First, the Xgboost machine learning model was used to predict and generate the AGB map of PDF using airborne LiDAR height and intensity predictors. Second, the LiDAR-derived raster was used to create training/testing samples. In order to include a complete range of AGB values, a stratified random sampling method was used. Thus, pixels of LiDAR AGB raster were sorted from 0 to maximum AGB with 5 Mg/ha bins. Then, 200 pixels/ objects were randomly chosen within each bin. One-half of samples were selected when the bin had less than 200 pixels/objects (Hudak et al. 2020). For the OBIA approach, the boundaries were overlaid on LiDAR-derived raster to calculate the mean AGB of the object. Finally, 4,533 pixels and 4,266 objects were produced as training/testing samples for pixel-based and object-based techniques, respectively. The reference dataset was divided to 70% for training and 30% for testing. The performance of the final model was evaluated using the root mean square error (RMSE), R squared (R^2), and mean bias error (MBE) (Equations 3-5).

$$RMSE = \sqrt{\sum_{i=1}^{n} \frac{(\hat{y}_i - y_i)^2}{n}} \qquad (3)$$

$$R^2 = 1 - \frac{\sum_i (y_i - \hat{y}_i)^2}{\sum_i (y_i - \bar{y})^2} \qquad (4)$$

$$MBE = \frac{1}{n} \sum_{i=1}^{n} (y_i - \hat{y}_i) \qquad (5)$$

where $\hat{y}_i$ are predicted values
y_i are observed values
n is the number of observations
$\bar{y}$ is the mean of y values

3.3 Object-based Image Analysis (OBIA)

One of the most common feature extraction techniques in remote sensing image classification is OBIA approach (Blaschke 2010). This technique clusters pixels into objects based on their spectral similarity (Addink and Coillie 2010). Reducing the mixed pixels issues which exists in pixel-based approach is one of the advantages of OBIA (Salehi, Daneshfar, and Davidson 2017). As mentioned earlier, this method has not been used widely for forest AGB estimation. Thus, this study focuses on comparing pixel-based and object-based results for AGB prediction. The SNIC algorithm which is provided by GEE (Achanta and Susstrunk 2017) was used to segment forest canopies into similar objects using Sentinle-2 imagery (Figure 3). SNIC segmentation parameters (i.e. size, compactness, connectivity, neighborhoodSize, and seeds (Tassi and Vizzari 2020)) were selected based on trial and error and size of objects. The parameters were set as follows: size=5, compactness=0.1, connectivity=8, neighborhoodSize=60, and seeds=10.

After defining the optimum objects, some spectral and textural features were extracted as input predictors for AGB estimation. Mean and variance were the spectral and for textural features, angular second moment (ASM), contrast, entropy, and homogeneity were selected among available GLCM features in GEE.
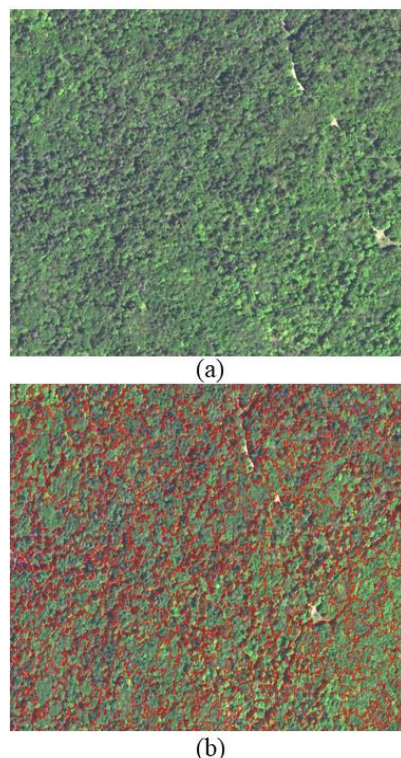

(a)

(b)

Figure 3. OBIA using the SNIC segmentation in GEE. (a) Imagery of a zoomed area, (b) boundaries of segmented objects.

4. RESULTS AND DISCUSSION

4.1 Tuning of Xgboost parameters

Table 2 shows the winning parameters after hyperparameter tuning using a grid search approach. Based on the hyperparameter tuning procedure, the Xgboost regression model is relatively neutral to the gamma value. In addition, when considering the same value of minimum_child_weight and maximum depth, the RMSE and R^2 does not change. To keep the RMSE results low, a higher value of minimum_child_weight is needed when the maximum depth increases. A lower value of learning rate decreases the contribution of each tree which prevents over-fitting issue (Li et al. 2020).

Parameter	Pixel-based	Object-based
nrounds	200	500
learning_rate	0.2	0.2
max_depth	4	6
eta	0.3	0.1
gamma	0.3	0
subsample	0.7	0.7
min_child_weight	1	5

Table 2. Wining values of hyperparameter tuning of Xgboost model using a grid search approach and optical + SAR data.

4.2 Pixel-based vs. Object-based using Xgboost model

Table 3 summarizes the RMSE, MBE, and R^2 of Xgboost regression model for optical, SAR, optical + SAR data, separately, for both pixel-based and object-based approaches. First, OBIA outperforms pixel-based approach regardless of datasets. Object-based technique enhanced the RMSE of AGB prediction about 6.28 Mg/ha for optical + SAR, 6.17 Mg/ha for SAR, and 5.6 Mg/ha for optical data in comparison to the pixel-based approach. In the OBIA, pixels are categorized into objects based on similar reflectance value (Salehi, Zhang, and Zhong 2013). This helps reducing the error of prediction caused by mixed pixels in heterogenous forest landscapes. Thus, as the results demonstrate OBIA improves the performance of the AGB estimation.

In addition, several studies have emphasized the importance of OBIA for the enhancement of forest AGB estimation (Hirata et al. 2018; Silveira et al. 2019). However, finding the appropriate parameters for optimum objects is a critical task. Therefore, in this study, a trial and error method based on both RMSE and the shape of the objects was used to select best objects.

As listed in Table 3, in both scenarios, optical+SAR data provides the best AGB estimation by improving RMSE, MBE, and R^2. Then, optical, and SAR data are in the second and third place, respectively. The reason behind the better performance of optical data in comparison to SAR data might be because of the number of input predictors derived from spectral variables.

Most of the studies in forest AGB estimation have used optical imagery (Singh et al. 2012; Zhang et al. 2019; Li et al. 2020). While optical data provide valuable information low penetrability (Saatchi 2019; Coops et al. 2021) and saturation issue are the limitations of these images (Zhou et al. 2016). On the other hand, SAR datasets with longer wavelengths such as L-band and P-band are capable of penetrating forest canopies (Saatchi 2019). Moreover, they are sensitive to geometrical and physical characteristics of forest canopies. It is worth mentioning that SAR data are also suffering from saturation problem depending the density of the biomass (Zhou et al. 2016; Saatchi 2019). Thus, this paper used the combination of optical and SAR data to take advantage of chemical, molecular, geometrical, and physical information (Mahdianpari et al. 2019; Saatchi 2019; Li et al. 2020) provided by optical + SAR datasets. The results show the importance of using the integration of optical and SAR data for AGB estimation.

Model		Optical	SAR	Optical + SAR
Pixel-based	RMSE (Mg/ha)	42.24	51.28	40.97
	MBE (Mg/ha)	5.91	8.32	4.54
	R^2	0.72	0.58	0.73
Object-based	RMSE (Mg/ha)	36.64	45.11	34.69
	MBE (Mg/ha)	3.27	-4.38	1.43
	R^2	0.77	0.65	0.79

Table 3. Comparison of pixel-based and object-based PDF forest AGB estimation using Xgboost regression model for optical, SAR, and optical + SAR data.

4.3 Comparing AGB Maps of Pixel-based vs. Object-based

Both pixel-based and object-based AGB maps of PDF forest for the Xgboost model trained on LiDAR AGB raster are shown in Figures 4 and 5 using the optical + SAR data. A clear difference can be seen in the performance of pixel-based and object-based AGB maps. For instance, OBIA has led to a better result in distinguishing roads from other land cover types. Red lines, in the Figure 5, above the Hudson River show the roads (Figure 5, C) which were well estimated as low biomass areas.

Figure 5, A and B are two samples of high and low biomass regions. AGB maps, canopy covers with the same reflectance were categorized as the same objects resulting in more accurate AGB mapping using OBIA.
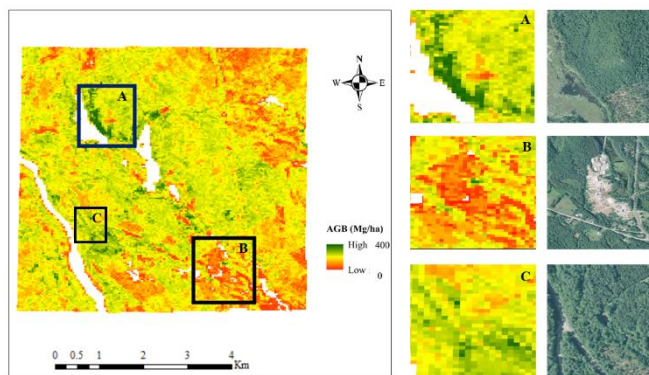

Figure 4. Pixel-based AGB map of PDF forest using Xgboost model and optical + SAR data trained on LiDAR-derived AGB raster
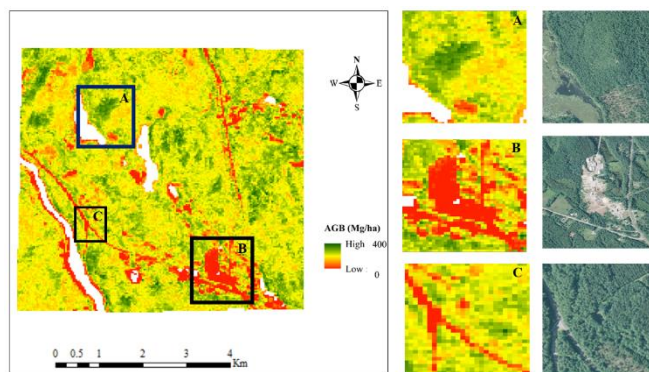

Figure 5. Object-based AGB map of PDF forest using Xgboost model and optical + SAR data trained on LiDAR-derived AGB raster

The comparison of pixel-based and object-based approaches demonstrated that OBIA presents more accurate AGB estimations and maps. First, PDF object-based AGB map looks smoother and the "salt-and-pepper" effect is less obvious. Second, the estimated AGB range of object-based approach is wider than pixel-based. This is due to the use of stratified sampling of LiDAR AGB raster as training datasets. The use of LiDAR AGB raster as training can significantly increase the amount of training samples, which improves the performance of machine learning training process.

5. CONCLUSION

This study compared pixel-based and object-based feature extraction approaches for AGB estimation. The Xgboost regression model was used to predict AGB of temperate PDF forest in New York State, USA. Multiple freely available optical

and SAR data and their combination were utilized to estimate the AGB. The results proved that the combination of different remote sensing sources can increase the performance of AGB estimation. Object-based approach significantly enhanced the RMSE, MBE, and R^2 in comparison to the conventional pixel-based method. It is recommended to take advantage of the new up-coming NASA Indian Space Research Organization (ISRO) Synthetic Aperture Radar (NISAR) data. This sensor provides data at two bands (L-band and S-band) which is suitable for dense forests.

REFERENCES

Achanta, Radhakrishna, and Sabine Susstrunk. 2017. "Superpixels and Polygons Using Simple Non-Iterative Clustering." In *Proceedings of the IEEE Conference on Computer Vision and Pattern Recognition*, 4651–60. https://doi.org/10.1109/CVPR.2017.520.

Addink, Elisabeth, and F. van Coillie. 2010. "Object-Based Image Analysis." *GIM International* 24 (1): 12–15.

Berninger, Anna, Sandra Lohberger, Matthias Stängel, and Florian Siegert. 2018. "SAR-Based Estimation of above-Ground Biomass and Its Changes in Tropical Forests of Kalimantan Using L-and C-Band." *Remote Sensing* 10 (6): 831. https://doi.org/10.3390/rs10060831.

Blaschke, Thomas. 2010. "Object Based Image Analysis for Remote Sensing." *ISPRS Journal of Photogrammetry and Remote Sensing* 65 (1): 2–16. https://doi.org/10.1016/j.isprsjprs.2009.06.004.

Boudreau, Jonathan, Ross F. Nelson, Hank A. Margolis, André Beaudoin, Luc Guindon, and Daniel S. Kimes. 2008. "Regional Aboveground Forest Biomass Using Airborne and Spaceborne LiDAR in Québec." *Remote Sensing of Environment* 112 (10): 3876–90. https://doi.org/10.1016/j.rse.2008.06.003.

Breitmeyer, B.W., M.K. Gooden, M.J. Appleby, R. Ash, and J. Rahn. 2019. Continuous Forest Inventory (CFI), 1970-2017, Long-term Forest Property Monitoring by State University of New York College of Environmental Science and Forestry, New York, USA ver 1. Environmental Data Initiative. https://doi.org/10.6073/pasta/5f2eb71d634b9ca1ec3c37effa557d33 (Accessed 2021-12-01).

Cao, Luodan, Jianjun Pan, Ruijuan Li, Jialin Li, and Zhaofu Li. 2018. "Integrating Airborne LiDAR and Optical Data to Estimate Forest Aboveground Biomass in Arid and Semi-Arid Regions of China." *Remote Sensing* 10 (4): 532. https://doi.org/10.3390/rs10040532.

Chen, Tianqi, and Carlos Guestrin. 2016. "Xgboost: A Scalable Tree Boosting System." In *Proceedings of the 22nd Acm Sigkdd International Conference on Knowledge Discovery and Data Mining*, 785–94. https://doi.org/10.1145/2939672.2939785.
Chen, Tianqi, Tong He, Michael Benesty, Vadim Khotilovich, Yuan Tang, Hyunsu Cho, Kailong Chen, et al. 2021. *Xgboost: Extreme Gradient Boosting* (version 1.5.0.2). https://doi.org/10.1145/2939672.2939785.

Clough, Brian J., Grant M. Domke, David W. MacFarlane, Philip J. Radtke, Matthew B. Russell, and Aaron R. Weiskittel. 2018. "Testing a New Component Ratio Method for Predicting Total Tree Aboveground and Component Biomass for Widespread Pine and Hardwood Species of Eastern US." *Forestry: An*

International Journal of Forest Research 91 (5): 575–88. https://doi.org/10.1093/forestry/cpy016.

Coops, Nicholas C., Piotr Tompalski, Tristan RH Goodbody, Martin Queinnec, Joan E. Luther, Douglas K. Bolton, Joanne C. White, Michael A. Wulder, Oliver R. van Lier, and Txomin Hermosilla. 2021. "Modelling Lidar-Derived Estimates of Forest Attributes over Space and Time: A Review of Approaches and Future Trends." *Remote Sensing of Environment* 260: 112477. https://doi.org/10.1016/j.rse.2021.112477.

Dang, An Thi Ngoc, Subrata Nandy, Ritika Srinet, Nguyen Viet Luong, Surajit Ghosh, and A. Senthil Kumar. 2019. "Forest Aboveground Biomass Estimation Using Machine Learning Regression Algorithm in Yok Don National Park, Vietnam." *Ecological Informatics* 50: 24–32. https://doi.org/10.1016/j.ecoinf.2018.12.010.

Deng, Songqiu, Masato Katoh, Qingwei Guan, Na Yin, and Mingyang Li. 2014. "Estimating Forest Aboveground Biomass by Combining ALOS PALSAR and WorldView-2 Data: A Case Study at Purple Mountain National Park, Nanjing, China." *Remote Sensing* 6 (9): 7878–7910. https://doi.org/10.3390/rs6097878.

Dube, Timothy, Onisimo Mutanga, Cletah Shoko, Sam Adelabu, and Tsitsi Bangira. 2016. "Remote Sensing of Aboveground Forest Biomass: A Review." *Tropical Ecology* 57 (May): 125–32.

Duncanson, Laura, Amy Neuenschwander, Steven Hancock, Nathan Thomas, Temilola Fatoyinbo, Marc Simard, Carlos A. Silva, John Armston, Scott B. Luthcke, and Michelle Hofton. 2020. "Biomass Estimation from Simulated GEDI, ICESat-2 and NISAR across Environmental Gradients in Sonoma County, California." *Remote Sensing of Environment* 242: 111779. https://doi.org/10.1016/j.rse.2020.111779.

Earth Resources Observation And Science (EROS) Center. 2017. "Sentinel." Tiff,jpg. U.S. Geological Survey. https://doi.org/10.5066/F76W992G.

Gorelick, Noel, Matt Hancher, Mike Dixon, Simon Ilyushchenko, David Thau, and Rebecca Moore. 2017. "Google Earth Engine: Planetary-Scale Geospatial Analysis for Everyone." *Remote Sensing of Environment* 202: 18–27. https://doi.org/10.1016/j.rse.2017.06.031.

Hawbaker, Todd J., Nicholas S. Keuler, Adrian A. Lesak, Terje Gobakken, Kirk Contrucci, and Volker C. Radeloff. 2009. "Improved Estimates of Forest Vegetation Structure and Biomass with a LiDAR-Optimized Sampling Design." *Journal of Geophysical Research: Biogeosciences* 114 (G2). https://doi.org/10.1029/2008JG000870.

Hemati, MohammadAli, Mahdi Hasanlou, Masoud Mahdianpari, and Fariba Mohammadimanesh. 2021. "A Systematic Review of Landsat Data for Change Detection Applications: 50 Years of Monitoring the Earth." *Remote Sensing* 13 (15): 2869. https://doi.org/10.3390/rs13152869.

Hirata, Yasumasa, Naoyuki Furuya, Hideki Saito, Chealy Pak, Chivin Leng, Heng Sokh, Vuthy Ma, Tsuyoshi Kajisa, Tetsuji Ota, and Nobuya Mizoue. 2018. "Object-Based Mapping of Aboveground Biomass in Tropical Forests Using LiDAR and Very-High-Spatial-Resolution Satellite Data." *Remote Sensing* 10 (3): 438. https://doi.org/10.3390/rs10030438.

Huang, Jianfeng, Xinchang Zhang, Qinchuan Xin, Ying Sun, and Pengcheng Zhang. 2019. "Automatic Building Extraction from High-Resolution Aerial Images and LiDAR Data Using Gated Residual Refinement Network." *ISPRS Journal of Photogrammetry and Remote Sensing* 151: 91–105. https://doi.org/10.1016/j.isprsjprs.2019.02.019.

Hudak, Andrew T., Patrick A. Fekety, Van R. Kane, Robert E. Kennedy, Steven K. Filippelli, Michael J. Falkowski, Wade T. Tinkham, Alistair MS Smith, Nicholas L. Crookston, and Grant M. Domke. 2020. "A Carbon Monitoring System for Mapping Regional, Annual Aboveground Biomass across the Northwestern USA." *Environmental Research Letters* 15 (9): 095003. https://doi.org/10.1088/1748-9326/ab93f9.

Issa, Salem, Basam Dahy, Taoufik Ksiksi, and Nazmi Saleous. 2020. "A Review of Terrestrial Carbon Assessment Methods Using Geo-Spatial Technologies with Emphasis on Arid Lands." *Remote Sensing* 12 (12): 2008. https://doi.org/10.3390/rs12122008.

Jafarzadeh, Hamid, Masoud Mahdianpari, Eric Gill, Fariba Mohammadimanesh, and Saeid Homayouni. 2021. "Bagging and Boosting Ensemble Classifiers for Classification of Multispectral, Hyperspectral and PolSAR Data: A Comparative Evaluation." *Remote Sensing* 13 (21): 4405. https://doi.org/10.3390/rs13214405.

Karlson, Martin, Madelene Ostwald, Heather Reese, Josias Sanou, Boalidioa Tankoano, and Eskil Mattsson. 2015. "Mapping Tree Canopy Cover and Aboveground Biomass in Sudano-Sahelian Woodlands Using Landsat 8 and Random Forest." *Remote Sensing* 7 (8): 10017–41. https://doi.org/10.3390/rs70810017.

Lee, Jong-Sen, Mitchell R. Grunes, and Gianfranco De Grandi. 1999. "Polarimetric SAR Speckle Filtering and Its Implication for Classification." *IEEE Transactions on Geoscience and Remote Sensing* 37 (5): 2363–73. https://doi.org/10.1109/36.789635.

Lee, Jong-Sen, and Eric Pottier. 2009. *Polarimetric Radar Imaging: From Basics to Applications*. CRC press.

Li, Chao, Mingyang Li, and Yingchang Li. 2020. "Improving Estimation of Forest Aboveground Biomass Using Landsat 8 Imagery by Incorporating Forest Crown Density as a Dummy Variable." *Canadian Journal of Forest Research* 50 (4): 390–98. https://doi.org/10.1139/cjfr-2019-0216.

Li, Manqi, Jungho Im, and Colin Beier. 2013. "Machine Learning Approaches for Forest Classification and Change Analysis Using Multi-Temporal Landsat TM Images over Huntington Wildlife Forest." *GIScience & Remote Sensing* 50 (4): 361–84. https://doi.org/10.1080/15481603.2013.819161.

Li, Yingchang, Chao Li, Mingyang Li, and Zhenzhen Liu. 2019. "Influence of Variable Selection and Forest Type on Forest Aboveground Biomass Estimation Using Machine Learning Algorithms." *Forests* 10 (12): 1073. https://doi.org/10.3390/f10121073.

Li, Yingchang, Mingyang Li, Chao Li, and Zhenzhen Liu. 2020. "Forest Aboveground Biomass Estimation Using Landsat 8 and Sentinel-1A Data with Machine Learning Algorithms." *Scientific Reports* 10 (1): 1–12. https://doi.org/10.1007/978-3-319-14708-6.

Li, Yingchang, Mingyang Li, Zhenzhen Liu, and Chao Li. 2020. "Combining Kriging Interpolation to Improve the Accuracy of Forest Aboveground Biomass Estimation Using Remote Sensing Data." *IEEE Access* 8: 128124–39. https://doi.org/10.1109/ACCESS.2020.3008686.

Mahdianpari, Masoud, Bahram Salehi, Fariba Mohammadimanesh, Saeid Homayouni, and Eric Gill. 2019. "The First Wetland Inventory Map of Newfoundland at a Spatial Resolution of 10 m Using Sentinel-1 and Sentinel-2 Data on the Google Earth Engine Cloud Computing Platform." *Remote Sensing* 11 (1): 43. https://doi.org/10.3390/rs11010043.

Næsset, Erik. 2011. "Estimating Above-Ground Biomass in Young Forests with Airborne Laser Scanning." *International Journal of Remote Sensing* 32 (2): 473–501. https://doi.org/10.1080/01431160903474970.

Pan, Bingyue. 2018. "Application of XGBoost Algorithm in Hourly PM2. 5 Concentration Prediction." In *IOP Conference Series: Earth and Environmental Science*, 113:012127. IOP publishing. https://doi.org/10.1088/1755-1315/113/1/012127.

Pesantez-Narvaez, Jessica, Montserrat Guillen, and Manuela Alcañiz. 2019. "Predicting Motor Insurance Claims Using Telematics Data—XGBoost versus Logistic Regression." *Risks* 7 (2): 70. https://doi.org/10.3390/risks7020070.

Pham, Tien Dat, Nga Nhu Le, Nam Thang Ha, Luong Viet Nguyen, Junshi Xia, Naoto Yokoya, Tu Trong To, Hong Xuan Trinh, Lap Quoc Kieu, and Wataru Takeuchi. 2020. "Estimating Mangrove Above-Ground Biomass Using Extreme Gradient Boosting Decision Trees Algorithm with Fused Sentinel-2 and ALOS-2 PALSAR-2 Data in Can Gio Biosphere Reserve, Vietnam." *Remote Sensing* 12 (5): 777. https://doi.org/10.3390/rs12050777.

Saatchi, Sassan. 2019. "SAR Methods for Mapping and Monitoring Forest Biomass." *Book: Flores A, Herndon K, Thapa R, Cherrington E, Eds. SAR Handbook: Comprehensive Methodologies for Forest Monitoring and Biomass Estimation*, 207–46.

Salehi, Bahram, Bahram Daneshfar, and Andrew M. Davidson. 2017. "Accurate Crop-Type Classification Using Multi-Temporal Optical and Multi-Polarization SAR Data in an Object-Based Image Analysis Framework." *International Journal of Remote Sensing* 38 (14): 4130–55. https://doi.org/10.1080/01431161.2017.1317933.

Salehi, Bahram, Yun Zhang, and Ming Zhong. 2013. "A Combined Object-and Pixel-Based Image Analysis Framework for Urban Land Cover Classification of VHR Imagery." *Photogrammetric Engineering & Remote Sensing* 79 (11): 999–1014. https://doi.org/10.14358/PERS.79.11.999.

Silveira, Eduarda MO, Sergio Henrique G. Silva, Fausto W. Acerbi-Junior, Monica C. Carvalho, Luis Marcelo T. Carvalho, Jose Roberto S. Scolforo, and Michael A. Wulder. 2019. "Object-Based Random Forest Modelling of Aboveground Forest Biomass Outperforms a Pixel-Based Approach in a Heterogeneous and Mountain Tropical Environment." *International Journal of Applied Earth Observation and Geoinformation* 78: 175–88. https://doi.org/10.1016/j.jag.2019.02.004.

Singh, Kunwar K., John B. Vogler, Douglas A. Shoemaker, and Ross K. Meentemeyer. 2012. "LiDAR-Landsat Data Fusion for Large-Area Assessment of Urban Land Cover: Balancing Spatial Resolution, Data Volume and Mapping Accuracy." *ISPRS Journal of Photogrammetry and Remote Sensing* 74: 110–21. https://doi.org/10.1016/j.isprsjprs.2012.09.009.

Siry, Jacek P., Frederick W. Cubbage, and Miyan Rukunuddin Ahmed. 2005. "Sustainable Forest Management: Global Trends and Opportunities." *Forest Policy and Economics* 7 (4): 551–61. https://doi.org/10.1016/j.forpol.2003.09.003.

Tassi, Andrea, and Marco Vizzari. 2020. "Object-Oriented LULC Classification in Google Earth Engine Combining SNIC, GLCM, and Machine Learning Algorithms." *Remote Sensing* 12 (22): 3776. https://doi.org/10.3390/rs12223776.

Urbazaev, Mikhail, Christian Thiel, Felix Cremer, Ralph Dubayah, Mirco Migliavacca, Markus Reichstein, and Christiane Schmullius. 2018. "Estimation of Forest Aboveground Biomass and Uncertainties by Integration of Field Measurements, Airborne LiDAR, and SAR and Optical Satellite Data in Mexico." *Carbon Balance and Management* 13 (1): 1–20. https://doi.org/10.1186/s13021-018-0093-5.

Watson, Robert T., Marufu C. Zinyowera, Richard H. Moss, and David Jon Dokken. 1998. *The Regional Impacts of Climate Change: An Assessment of Vulnerability*. Cambridge University Press.

Woodall, Christopher W., Linda S. Heath, Grant M. Domke, and Michael C. Nichols. 2011. "Methods and Equations for Estimating Aboveground Volume, Biomass, and Carbon for Trees in the US Forest Inventory, 2010." https://doi.org/10.2737/NRS-GTR-88.

Wulder, Michael A., Nicholas C. Coops, Andrew T. Hudak, Felix Morsdorf, Ross Nelson, G. Newnham, and Mikko Vastaranta. 2013. "Status and Prospects for LiDAR Remote Sensing of Forested Ecosystems." *Canadian Journal of Remote Sensing* 39 (sup1): S1–5. https://doi.org/10.5589/m13-051.

Yue, Jibo, Guijun Yang, Qingjiu Tian, Haikuan Feng, Kaijian Xu, and Chengquan Zhou. 2019. "Estimate of Winter-Wheat above-Ground Biomass Based on UAV Ultrahigh-Ground-Resolution Image Textures and Vegetation Indices." *ISPRS Journal of Photogrammetry and Remote Sensing* 150: 226–44. https://doi.org/10.1016/j.isprsjprs.2019.02.022.

Zhang, Rong, Xuhui Zhou, Zutao Ouyang, Valerio Avitabile, Jiaguo Qi, Jiquan Chen, and Vincenzo Giannico. 2019. "Estimating Aboveground Biomass in Subtropical Forests of China by Integrating Multisource Remote Sensing and Ground Data." *Remote Sensing of Environment* 232: 111341. https://doi.org/10.1016/J.RSE.2019.111341.

Zhou, Xudong, Xinkai Zhu, Zhaodi Dong, and Wenshan Guo. 2016. "Estimation of Biomass in Wheat Using Random Forest Regression Algorithm and Remote Sensing Data." *The Crop Journal* 4 (3): 212–19. https://doi.org/10.1016/j.cj.2016.01.008.
Zhu, Yan, Zhongke Feng, Jing Lu, and Jincheng Liu. 2020. "Estimation of Forest Biomass in Beijing (China) Using Multisource Remote Sensing and Forest Inventory Data." *Forests* 11 (2): 163.